4392–4404 *Nucleic Acids Research, 2018, Vol. 46, No. 9* *Published online 27 February 2018*
doi: 10.1093/nar/gky149

Stabilization of the methyl-CpG binding protein ZBTB38 by the deubiquitinase USP9X limits the occurrence and toxicity of oxidative stress in human cells

Benoit Miotto[1,2,*,†], Claire Marchal[1,2,†], Guillaume Adelmant[3], Nadège Guinot[2], Ping Xie[4], Jarrod A. Marto[3], Lingqiang Zhang[4] and Pierre-Antoine Defossez[1,*]

[1]Univ. Paris Diderot, Sorbonne Paris Cité, Epigenetics and Cell Fate, UMR 7216 CNRS, 75013 Paris, France, [2]Institut Cochin, Sorbonne Paris Cité, 75014 Paris, France, [3]Department of Cancer Biology, Dana-Farber Cancer Institute, Boston, MA 02115, USA; Department of Biological Chemistry and Molecular Pharmacology, Harvard Medical School, Boston, MA 02115, USA; Blais Proteomics Center, Dana-Farber Cancer Institute, Boston, MA 02115, USA and [4]State Key Laboratory of Proteomics, National Center of Protein Science (Beijing), Beijing Institute of Lifeomics, Beijing 100850, China

Received January 05, 2018; Revised February 05, 2018; Editorial Decision February 15, 2018; Accepted February 16, 2018

ABSTRACT

Reactive oxygen species (ROS) are a byproduct of cell metabolism, and can also arise from environmental sources, such as toxins or radiation. Depending on dose and context, ROS have both beneficial and deleterious roles in mammalian development and disease, therefore it is crucial to understand how these molecules are generated, sensed, and detoxified. The question of how oxidative stress connects to the epigenome, in particular, is important yet incompletely understood. Here we show that an epigenetic regulator, the methyl-CpG-binding protein ZBTB38, limits the basal cellular production of ROS, is induced by ROS, and is required to mount a proper response to oxidative stress. Molecularly, these functions depend on a deubiquitinase, USP9X, which interacts with ZBTB38, deubiquitinates it, and stabilizes it. We find that USP9X is itself stabilized by oxidative stress, and is required together with ZBTB38 to limit the basal generation of ROS, as well as the toxicity of an acute oxidative stress. Our data uncover a new nuclear target of USP9X, show that the USP9X/ZBTB38 axis limits, senses and detoxifies ROS, and provide a molecular link between oxidative stress and the epigenome.

INTRODUCTION

The cells in our bodies constantly undergo oxidative challenge from endogenous and exogenous sources (1). This is not necessarily detrimental: oxidative stress within a physiological range, or 'eustress', is actually important for proper mammalian physiology, as well demonstrated in the skin (2) or the immune system (3) for instance. In contrast, excessive amounts of oxidative stress, or improper cellular response to the stress, is linked to cellular senescence, organismal aging, and a number of diseases including cancers (1). For these reasons, it is important to understand the cellular mechanisms that generate, sense, and counteract oxidative stress.

Some of these molecular pathways have already been well delineated, and a pivotal actor is the KEAP1/NRF2 axis. KEAP1 is an adaptor protein for E3 ubiquitin ligases which maintains a low steady-state level of the NRF2 protein. Under oxidative stress, the oxidation of critical cysteines inactivates KEAP1 and stabilizes NRF2, which can then activate a transcriptional program containing key antioxidant actors (4,5). In spite of these and other important advances, our understanding of the molecular pathways responding to oxidative stress remains incomplete. One particular area that has yet to be fully understood is the link between oxidative stress and epigenetics.

Oxidative stress alters the epigenome and in particular DNA methylation. A direct molecular explanation is that reactive oxygen species (ROS) can modify methylated CpGs (6) and prevent their interaction with some of the tran-

*To whom correspondence should be addressed. Tel: +33 1 57 27 89 16; Email: pierre-antoine.defossez@univ-paris-diderot.fr
Correspondence may also be addressed to Benoit Miotto. Tel: +33 1 44 41 24 35; Email: benoit.miotto@inserm.fr
†These authors contributed equally to this work as first authors.
Present address: Ping Xie, Department of Biochemistry and Molecular Biology, Capital Medical University, Beijing 100069, China.

scriptional regulators that normally recognize them. However, the ∼20 million methylated cytosines in a nucleus (7) vastly outnumber the number of molecules of methyl-CpG-binding proteins (typically ∼100 000, (8)), therefore this mechanism probably only applies at very high, and possibly physiologically irrelevant, ROS concentrations. This suggests that other mechanisms may link oxidative stress and methylated DNA.

We and others have previously demonstrated that the human protein ZBTB38 recognizes methylated DNA via its Zinc fingers (9–11). We have further shown that ZBTB38 is important for genome stability (12) and, independently, polymorphisms in ZBTB38 have been shown to have strong genetic links to the risk for men to develop prostate cancer (13). To better understand the functions of ZBTB38 we have carried out an unbiased proteomic search for its interactors.

Here, we present the ZBTB38 interactome and report that ZBTB38 interacts with the deubiquitinase USP9X; that this interaction controls the stability of ZBTB38; that both proteins are coordinately stabilized by oxidative stress; that together they control the basal level of ROS in cells; and that together they are necessary for cells to mount a proper response to oxidative stress. In summary, we identify a new axis regulating the cellular response to oxidative stress, and this axis links oxidative stress with protein stability and DNA methylation in novel ways.

MATERIALS AND METHODS

Cell lines and culture conditions

The colon cancer HCT116 (p53+/+) and HCT116 (p53–/–) cells were kindly provided by Dr Bert Vogelstein. The cells were cultured in McCoy's 5A modified media (Thermo Fisher Scientific) supplemented with 10% fetal bovine serum. The human U2OS and HeLa cells were cultured in Dulbecco's modified Eagle's medium (DMEM) (Thermo Fisher Scientific) supplemented with 10% fetal bovine serum.

Construction of the HeLa S3 cell line expressing HA-Flag-ZBTB38

The cDNA encoding ZBTB38 was PCR amplified and cloned into the pREV lentiviral vector, kindly provided by S. Ait-Si-Ali. The plasmid contains an epitope tag (3xHA- and 3xFlag-tag) in 5′ of the cloning site and a selection marker. We validated the expression of HA-Flag-ZBTB38 in selected cells following infection. We further validated the functionality of the tagged protein by a recruitment test on chromocenters in murine cells and performing a co-immunoprecipitation of ZBTB38 partners in human cells. We eventually selected a HeLa S3 XLP cell line expressing ZBTB38 at similar level to the endogenous protein. HeLa HA-Flag-ZBTB38 were grown in DMEM supplemented with 10% foetal bovine serum and Penicillin/Streptomycin.

TAP-tag purification of HA-Flag-ZBTB38 and identification of ZBTB38 partners by mass-spectrometry

Soluble nuclear extracts were prepared, and HA-Flag-ZBTB38 was immunoprecipitated following the protocol previously described in detail (14). Tandem Affinity Purified UHRF1 samples were reduced with 10 mM DTT for 30 min at 56°C in the presence of 0.1% RapiGest SF (Waters). Cysteines were alkylated with 22.5 mM iodoacetamide for 20 min at room temperature in the dark. Samples were digested overnight at 37°C with 4 ug trypsin (Promega). Tryptic peptides were acidified and purified by batch mode reversed phase and strong cation exchange chromatography (15). Purified peptides were divided in two aliquots and analyzed in two independent nanoLC-MS runs (16). Peptides were loaded onto a precolumn (4 cm POROS 10R2, Applied Biosystems) and eluted with an HPLC gradient (NanoAcquity UPLC system, Waters; 2–35% B in 45 min; A = 0.2 M acetic acid in water, B = 0.2 M acetic acid in acetonitrile). Peptides were resolved on a self-packed analytical column (12 cm Monitor C18, Column Engineering) and introduced in the mass spectrometer (LTQ Orbitrap Velos, Thermo Scientific) equipped with a Digital PicoView electrospray source platform (New Objective, ESI spray voltage = 2.2 kV). The mass spectrometer was programmed to perform data-dependent MS/MS on the 10 most abundant precursors in each MS1 scan using alternating collision induced and higher energy dissociation (CID and HCD respectively, with 35% normalized collision energy). Dynamic exclusion was enabled with a repeat count of one and exclusion duration of 30 s. MS spectra were recalibrated using the background ion (Si(CH3)2O)6 at m/z 445.12 ± 0.03 and converted into a Mascot generic file format (.mgf) using multiplierz scripts (17). Search parameters included trypsin specificity with up to two missed cleavages, fixed carbamidomethylation (C, +57 Da) and variable oxidation (M, +16 Da). Precursor mass tolerance was set to 15 ppm and product ion mass tolerances were set to 0.6 Da and 0.02 Da for CID and HCD spectra, respectively. The search databases consisted of human protein sequences (downloaded from RefSeq on 7 November 2011) and protein sequences for common lab contaminants both appended to their own decoy database. Sequence matches to the decoy databases were used to implement a global 1% false discovery rate (FDR) filter for the resulting peptide identifications. A fast peptide matching algorithm was used to map peptide sequences to all possible human genes. We discarded candidate proteins that were detected in a large compendium of negative TAP controls with a frequency >1% (18).

Proximity ligation assay

In situ proximity ligation assays were performed using the Duolink® PLA® technology (Sigma Aldrich #DUO92014) on paraformaldehyde fixed cells. We used PLA probe PLUS for primary mouse antibodies (Sigma Aldrich #DUO92001) and PLA probe MINUS for rabbit primary antibodies (Sigma Aldrich #DUO92005). The PLA reaction was performed as described in the brochure. Cells were mounted in vectashield with DAPI (Vector laboratories #H-1200).

GST pull-down assay

Glutathion Sepharose Beads (Life Technologies #G2879) coated with GST-fusion proteins, representing different domains of ZBTB38, were incubated with a cellular extract

prepared from cells expressing USP9X. After incubation and several washes, the amount of USP9X retained by each ZBTB38-fragment was analyzed by western blotting. We followed a previously established protocol (12).

Co-immunoprecipitation analysis

Total protein extract were prepared by mixing cells with lysis buffer (400 mM KCl, 20 mM Tris–HCl (pH 7.5), 20% glycerol, 5 mM DTT, 0.4 mM PMSF). The protein extract was then adjusted to 1 ml at 100 mM KCl cell lysis buffer. The extract was incubated for 2 h in a cold room with agitation in the presence of the ZBTB38 antibody produced in rabbit or the USP9X antibody produced in mouse. The Sepharose beads coupled with protein A/G were then added for an additional 2 h and recovered by centrifugation and washed three times with 1 ml of RIPA buffer (1 × PBS, 0.1% SDS, 0.5% sodium deoxycholate, 0.5% NP-40). The adsorbed proteins were dissociated by boiling for 5 min in 20 μl of Laemmli buffer and resolved by SDS–polyacrylamide gel electrophoresis. Proteins separated by electrophoresis were electro-transferred onto a nitrocellulose filter.

siRNA transfection

The different siRNAs were purchased from Thermo Fisher Scientific: negative control (12935300) or directed against ZBTB38 (HSS153846, HSS153847), USP9X (HSS112072, HSS112073) and USP7 (HSS111817, HSS111818). Transfections of siRNA were performed using Lipofectamine 2000, according to the manufacturer's instructions.

Gene expression analysis

RT-qPCR have been performed as previously described (12). The primers used are USP9X (TCG GAG GGA ATG ACA ACC AG and GGA GTT GCC GGG GAA TTT TCA), ZBTB38 (GGT GTG ACA TCT CAT GTG CAT T and AAG GCC CCA CCG ACA TCT TA), USP7 (TCT GAT TCC ACG TCA TGG TCT and CGA CGA CTG AAC GAC TTT TCA TC), MAPK14 (TGC CGA AGA TGA ACT TTG CGA and TCA TAG GTC AGG CTT TTC CAC T), TBP (CCA CTC ACA GAC TCT CAC AAC and CTG CGG TAC AAT CCC AGA ACT) and TFRC (ACC ATT GTC ATA TAC CCG GTT CA and GGC CTT TGT GTT ATT GTC AGC AT).

Cell treatments

For experiments on synchronized cells, cells were treated for 12 hours with nocodazole (0.1 μg/ml, Mitosis arrest) or hydroxyurea (100 μM, S-phase arrest). Treatments used on cells were: MG132 (20 mM, 8 h), WP1130 (2 μM, 2 h), H_2O_2 (as indicated in legends), etoposide (200 μM, 1 h), HU (2 mM, 2 h), except when different conditions are described in legends. Conditioned media was obtained by treating cells with H_2O_2, harvesting and filtering the media, and using this fresh media on cells to analyze. Irradiations of cell samples were performed at Curie Institute using a Cesium 137 irradiator (Institut Curie, Paris, France). Recombinant SOD, PEG-SOD, Catalase and PEG-Catalase were added to the culture media 1 h prior to H_2O_2 addition. All molecules were used at final concentration of 50 U/ml.

Ubiquitination level assessment

We measured ubiquitin enrichment by using the ubiquitin enrichment kit (ThermoFischer Scientist #1859662), according to the manufacturer's protocol.

Colony forming assay

A fixed number of adherent cells (200 cells) were seeded in 6-well plates. After 24 h in the incubator the cells were exposed to different concentrations of the reagents of interest. After treatment, the culture media was changed every 2–3 days, for 2 weeks. The cells were then washed with PBS, and incubated in crystal violet solution (0.05% crystal violet, 1% formaldehyde in H_2O) for 30 min. Plates were then washed five times with H_2O and photographed. The ratio between the number of colonies in the treated condition normalized to the number of colonies in the control condition is reported in the graphs.

Measure of antioxidant activity

The antioxidant assay was performed as described by the manufacturer (Antioxidant assay kit; CS0790; Sigma). Briefly, 10^7 HeLa or U2OS cells treated with relevant siRNAs, combination of siRNAs or plasmids were lysed in assay buffer. Twenty microliters of lysate were then mixed with adequate volumes of myoglobin working solution and ABTS substrate working solution. After 5 min incubation at room temperature, the reaction was stopped by adding Stop solution and the endpoint absorbance read at 405 nm. The level of antioxidant was then reported in the figures as the fold over the control condition.

Measure of reactive oxygen species accumulation

2′,7′-Dichlorofluorescin diacetate (DCF-DA) and dihydroethidium (DHE) were purchased from Sigma (D6883 and D7008). DCF-DA was used at a final concentration of 20 μmpl for 30 minutes in PBS. DHE was used at a final concentration of 1 mM for 20 min in PBS. The fluorescence intensity per cell was then analyzed using the BDbiosciences FACSCalibur platform and the mean fluorescence per samples determined using the BD CellQuest™ Pro software. Twenty thousand cells were analyzed per condition.

Cell death analysis

The estimation of cell death in samples was determined using three independent assays, namely trypan blue exclusion assay, propidium iodide intake and FACS analysis (i.e. sub-G1 proportion; 19-20). The trypan blue exclusion assay was performed according to manufacturer guidelines (Life Technologies; 15250-061). Under a microscope, 300 cells were scored for live (unstained) and dead (blue) cells. The propidium iodide (Sigma #P4170) intake assay was conducted as previously described (21) using a BD biosciences FACSCalibur platform and the BD CellQuest Pro software

for data analysis. Ten thousand cells were analyzed per condition. The sub-G1 cell population was obtained from the analysis of the cell cycle profile. Ten thousand cells were analyzed per condition.

Antibodies

References of primary antibodies used in this study are: ZBTB38 (homemade antibody #148), USP9X (Millipore #MABE352; Abcam #19879; Bethyl Lab #A301-351A), GST (CST #2622), GAPDH (Abcam #ab9485), USP7 (Abcam #4080), HA (CST,#2367), H2AX (Bethyl Lab #A300-083A), phospho-H2AX (Millipore #05–636), TUBULIN (Abcam #ab7291), RFP (Rockland #600-401-379), V5 (Santa Cruz #sc-84594), MYC (CST #2276), WEE1 (Abcam #79298), NRF2 (Abcam #ab62352), PGC1 (Abcam #72230), DNMT1 (Imgenex #IMG-261A), ORC2 (Santa Cruz #28742), phospho-CHK1 (CST #2341), phospho-CHK2 (CST #2661), phospho-ATM (CST #4526P), PARP1 (CST #9542), JNK (Santa Cruz #474) and 53BP1 (Abcam #21083).

RESULTS

ZBTB38 interacts with USP9X in the nucleus

We and others have previously shown that the ZBTB38 protein is unstable and is regulated by a ubiquitin/proteasome-dependent pathway (12,22). To further understand the regulation and roles of ZBTB38 we used a biochemical approach, designed to identify the ZBTB38 protein complexes present in human cells. A stable HeLa cell line expressing an HA- and Flag-tagged version of ZBTB38 was established. The tagged protein was found to reside in the nucleus, like its endogenous counterpart, to migrate at the expected size, and to have an abundance inferior to that of the endogenous protein (Supplementary Figure S1A and B). We then used affinity purification to isolate ZBTB38 complexes from soluble nuclear extracts, inspected them visually by SDS-PAGE, and analyzed them by mass spectrometry (Figure 1A and B, Supplemental Table S1). Two biological replicates of the complexes were isolated and analyzed, and two deubiquitinases were present in both replicates: USP9X and USP7 (Figure 1B, Supplemental Table S1). Both enzymes were absent from the immunoprecipitation carried out on cells not expressing HA-Flag-ZBTB38 and from other protein complexes isolated by the same procedure (14). This suggests that these deubiquitinases could be specifically associated with ZBTB38, and might be involved in its regulation.

In order to confirm the interaction between endogenous USP9X and ZBTB38, co-immunoprecipitation was then carried out with HeLa nuclear lysates; we found that USP9X was indeed enriched in ZBTB38 immunoprecipitates (Figure 1C). This experiment was performed in the presence of Ethidium Bromide, ruling out the possibility that the interaction was bridged by DNA. We thus conclude from these experiments that USP9X interacts with ZBTB38 in the nucleus of human cells. Further support for this result was obtained by an independent method: Proximity Ligation Assay (PLA). We observed the presence of fluorescent dots, establishing the physical nearness of USP9X and ZBTB38, only when the specific antibodies against USP9X and ZBTB38 were combined (Figure 1D). Furthermore, the majority of dots were nuclear, suggesting that the interaction between USP9X and ZBTB38 occurred mostly in the nucleus. Using *in vitro* pull-down assays we delineated the regions of the proteins involved in the interaction: this showed that a central region of ZBTB38 (amino acids: 598–945) was required for the interaction (Figure 1E).

From these data, we conclude that USP9X and ZBTB38 interact, and that this interaction occurs mostly in the nucleus.

ZBTB38 protein abundance is regulated by USP9X

USP9X can stabilize the proteins it interacts with (see for instance ref. 23). To determine if this applies to ZBTB38, we knocked down USP9X with siRNAs. In all cell lines tested (HeLa, HCT116, HCT116 $p53^{-/-}$, U2OS), ZBTB38 protein abundance was found to be lower in USP9X-depleted cells compared to control siRNA-treated cells (Figure 2A and Supplementary Figure S2A). In addition, ZBTB38 mRNA was equally abundant in USP9X-depleted and control cells, showing that the effect was post-transcriptional (Figure 2A and Supplementary Figure S2A). We also knocked down USP7, the other deubiquitinase found in the ZBTB38 complex; this had no consequence on either ZBTB38 mRNA or protein abundance, establishing that only certain deubiquitinases control ZBTB38 stability (Supplementary Figure S2B). We noticed that ZBTB38 protein levels are regulated during the cell cycle: ZBTB38 expression was higher in S-phase cells (synchronized by hydroxyurea) than in M-phase cells (synchronized by nocodazole), and USP9X depletion significantly reduced ZBTB38 protein abundance in both cases (Figure 2B). These data indicate that the stabilization of ZBTB38 by USP9X is not restricted to a given phase of the cell cycle. Finally, we treated USP9X-depleted cells with a proteasome inhibitor, MG132, which increased the amount of ZBTB38 (Figure 2C), consistent with USP9X controlling ZBTB38 protein stability.

Altogether these results show that USP9X regulates ZBTB38 protein stability in human cells.

USP9X deubiquitinates ZBTB38

To further characterize the role of USP9X in ZBTB38 protein stability, we next investigated whether the enzymatic activity of USP9X was involved. We thus tested the effect of a chemical inhibitor of USP9X, WP1130 (24). After a 2-h treatment with WP1130, a strong down-regulation of ZBTB38 protein level was observed in different cell lines (Figure 2D) while no significant changes in mRNA level were detected (Figure 2E). Importantly, our short WP1130 treatment had no detectable consequence on the cell cycle distribution or on the cell survival, ruling out possible confounding effects (Figure 2F).

Next, we examined ZBTB38 ubiquitination. We expressed in cells an HA-tagged version of ubiquitin, treated the cells with MG132 to stabilize ubiquitinated proteins, immunoprecipitated the endogenous ZBTB38 protein, and assessed its ubiquitination level by western blotting with an antibody directed against the HA tag. When cells were

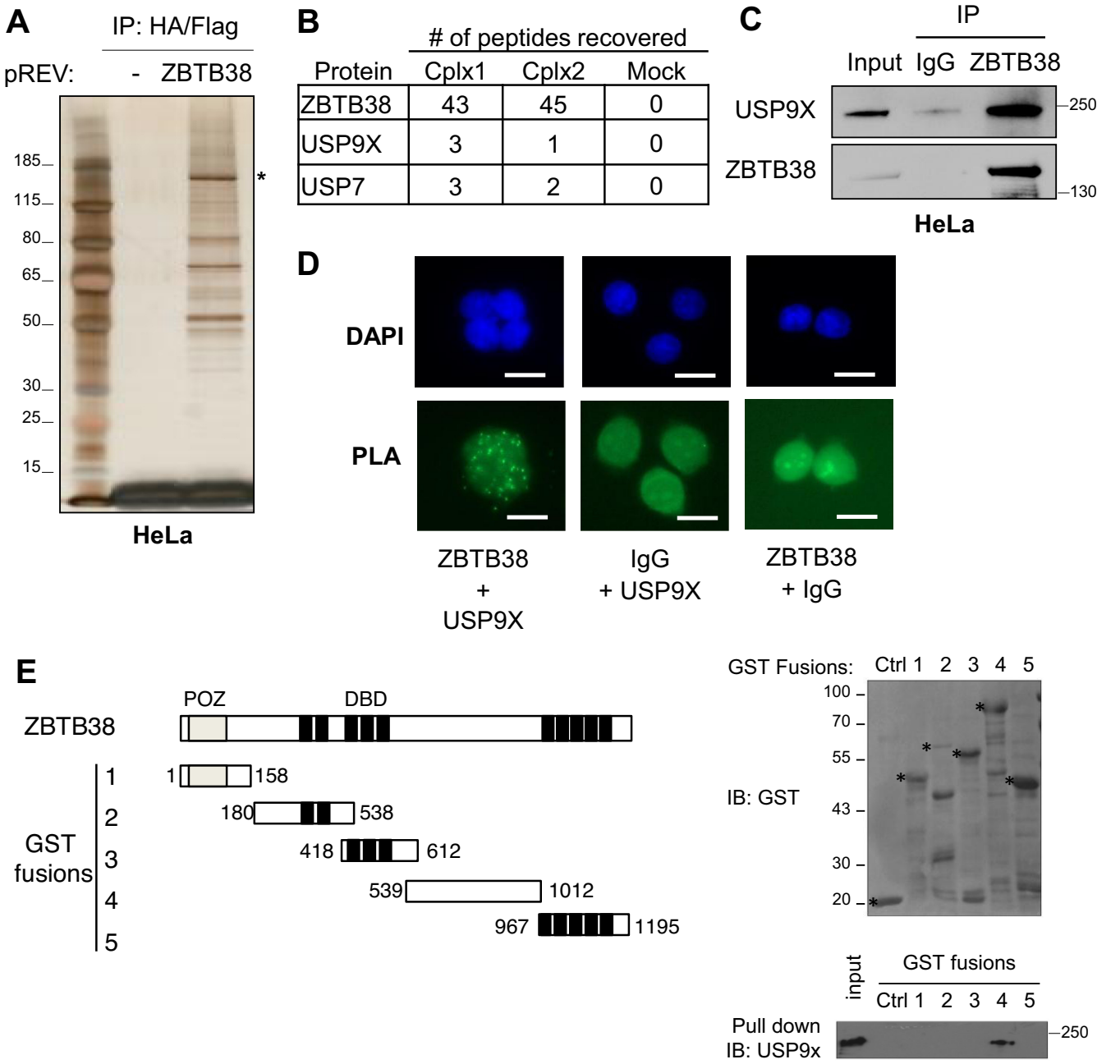

Figure 1. USP9X and ZBTB38 interact. (**A**) Silver staining of the purified HA-Flag-ZBTB38 complex. HeLa cells stably expressing an HA-Flag-ZBTB38 construct were lysed and the soluble nuclear fraction subjected to a TAP-Tag purification. The asterisk indicates the position of HA-Flag-ZBTB38. (**B**) Table showing the deubiquitinases recovered among ZBTB38 co-purifying proteins. The number of peptides recovered is indicated, as observed in two independent immunoprecipitations carried out on the HA-Flag-ZBTB38-expressing cells (Cplx1 and Cplx2) or on control cells (Mock). (**C**) Endogenous USP9X co-immunoprecipitates with endogenous ZBTB38 in HeLa cell nuclear extracts. (**D**) Proximity ligation assay confirms the juxtaposition of endogenous USP9X and endogenous ZBTB38 in HeLa cell nuclei. Green dots occur at sites of interaction. The cells were counter stained with DAPI to visualize the nucleus. Scale bar: 10μm. (**E**) A pull-down assay determines the USP9X-interacting region within ZBTB38. Left section: the domains of ZBTB38 produced as GST fusions and used in the assay (position of start and end amino acids indicated). Black boxes represent the C2H2 zinc fingers and the grey box represents the BTB/POZ domain. Top right section: western blotting with a GST antibody shows adequate expression of all the GST-ZBTB38 constructs (shown with an asterisk). 'Ctrl' denotes GST. Bottom right panel: HeLa nuclear extracts were incubated with the indicated GST fusion proteins, the complexes were bound to sepharose beads, washed, eluted and then probed for the presence of USP9X by western blotting. Construct #4 contains the interaction domain with USP9X.

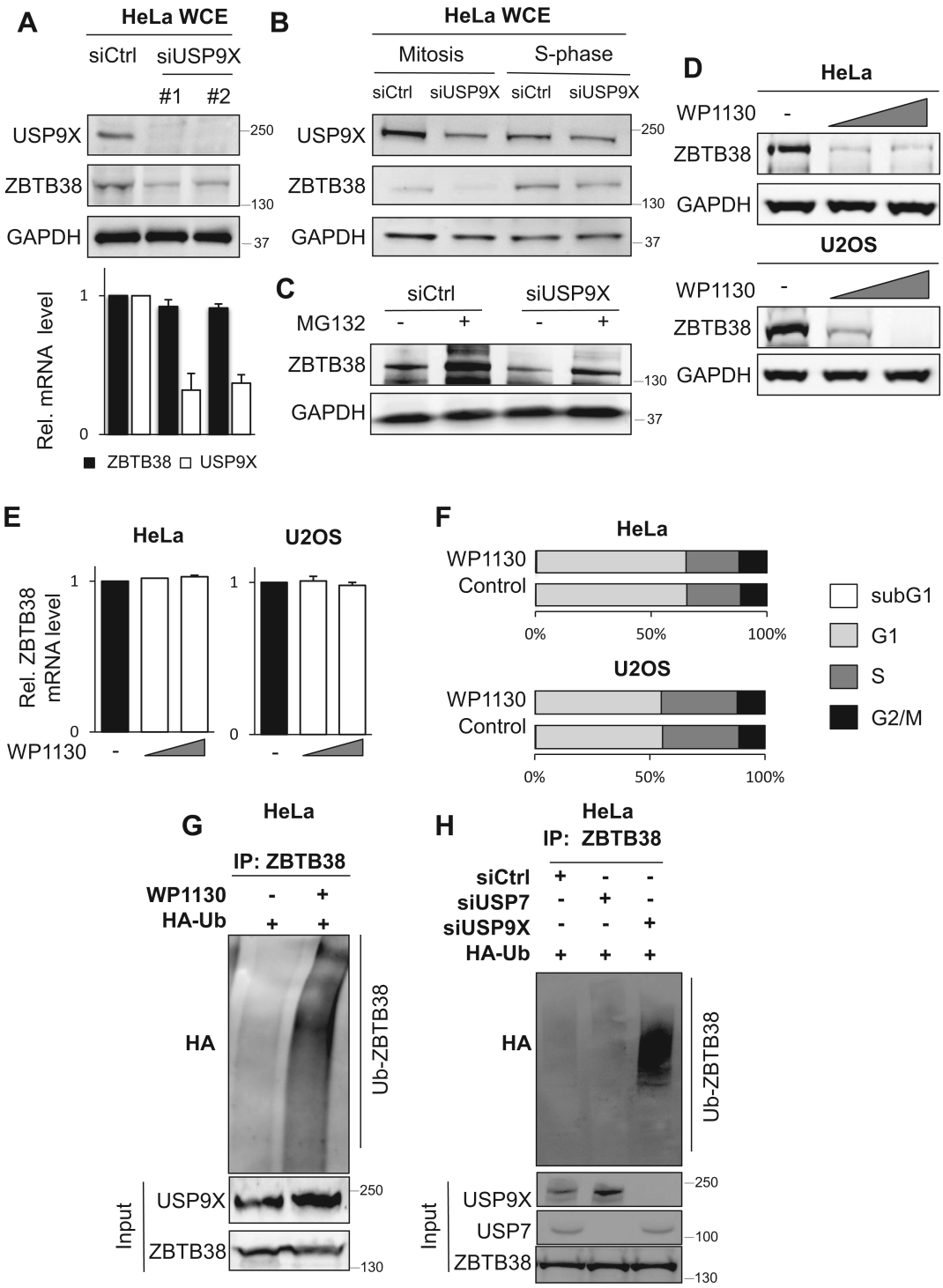

Figure 2. USP9X activity regulates ZBTB38 protein abundance. (**A**) Depletion of USP9X by siRNA causes a decrease in ZBTB38 protein abundance. Upper panel: western blot in HeLa cells; two independent siRNAs were used, GAPDH is a loading control. WCE: whole-cell extract. Lower panel: ZBTB38 mRNA abundance is not affected by USP9X depletion. qRT-PCR on HeLa cells after siRNA transfection, values normalized to three housekeeping genes (MAPK14, TBP and TFRC), $n = 3$. (**B**) The amount of ZBTB38 is cell-cycle regulated, and USP9X stabilizes ZBTB38 in both mitosis and S-phase. Western blotting on HeLa cells transfected with the indicated siRNAs, then synchronized in mitosis (with nocodazole), or in S-phase (with hydroxyurea). (**C**) ZBTB38 is stabilized by MG132 (20 mM, 8 h). Western blot as in panels A and B (**D**) Treatment with a USP9X inhibitor, WP1130, causes a decrease in ZBTB38 protein abundance. The cells were harvested immediately after a 2-h treatment with WP1130 (lower concentration: 1μM; higher concentration: 2μM), then western blotting was carried out with WCE. (**E**) Treatment with WP1130 does not affect ZBTB38 mRNA abundance. RT-qPCR as in panel A. (**F**) Treatment with WP1130 does not affect cell cycle distribution or viability, as determined by FACS analysis. (**G**) Treatment with WP1130 leads to an increase of ZBTB38 ubiquitination. Cells were tranfected with an HA-ubiquitin expression vector, treated with MG132 (20mM, 8hrs), and ubiquitinated ZBTB38 was precipitated followed by immunoblotting with anti-HA. (**H**) Depletion of USP9X, but not USP7, leads to an increase of ZBTB38 ubiquitination. As in panel G.

treated with WP1130, we observed much higher levels of ZBTB38 ubiquitination than in untreated cells (Figure 2G). The depletion of USP9X by siRNA also increased ZBTB38 poly-ubiquitination, whereas the depletion of USP7 had no effect (Figure 2H). We thus conclude that USP9X activity triggers the deubiquitination of ZBTB38 in cells.

We previously reported that the E3 ligase RBBP6 ubiquitinates and destabilizes ZBTB38 (12). We thus investigated the potential interplay between RBBP6 and USP9X activities. USP9X overexpression was found to rescue the destabilization of ZBTB38 caused by RBBP6 overexpression (Supplementary Figure S2C). Conversely, the depletion of USP9X further down-regulated the abundance of ZBTB38 protein in cells over-expressing RBBP6 (Supplementary Figure S2D). By poly-ubiquitination assays, we observed that USP9X causes deubiquitination of ZBTB38, even in cells over-expressing RBBP6 and conversely that inactivation of USP9X amplifies the polyubiquitination induced by RBBP6 over-expression (Supplementary Figure S2E and F).

Together these data show that USP9X deubiquitinates ZBTB38, both in basal conditions, and in conditions where ZBTB38 ubiquitination is augmented by RBBP6.

ZBTB38 accumulates following oxidative stress; this involves ROS and USP9X

Our next objective was to identify physiological conditions under which the regulation of ZBTB38 by USP9X may be important. For this, a number of experimental treatments were screened, including exposing the cells to oxidative stress by H_2O_2; we observed that this treatment triggered an accumulation of ZBTB38 protein (Figure 3A). The accumulation of ZBTB38 upon H_2O_2 treatment was observed in every cell line tested, independently of p53 or p21 status (Supplementary Figure S3A), and occurred without any detectable change in ZBTB38 mRNA level (Figure 3B and Supplementary Figure S3A). It is noteworthy that no ZBTB38 accumulation took place when cells were incubated with conditioned medium from cells exposed to H_2O_2 (Supplementary Figure S3B). This accumulation of ZBTB38 upon H_2O_2 treatment was not limited to a specific cell cycle stage, as it was noticeable both in S-phase and M-phase synchronized cells (Supplementary Figure S3C).

An independent treatment causing oxidative stress was also examined: ionizing radiation (IR); in this case an accumulation of ZBTB38 protein was also visible, without any change in mRNA level (Supplementary Figure S3D and S3E). Of note, IR exposure had no detectable effect on the level of expression of the related protein ZBTB33/KAISO (Supplementary Figure S3D).

We then asked whether ZBTB38 protein accumulation possibly reflected a cellular response to DNA damage caused by the ROS. First, we compared ZBTB38 protein accumulation and the level of histone H2AX phosphorylation, which parallels DNA damage, in cells treated with increasing H_2O_2 concentrations (Figure 3A). Within this treatment range (0–200 μM H_2O_2, 30 min treatment), no phospho-H2AX was dectectable, despite a clear accumulation of ZBTB38 protein (Figure 3A). Thus, we conclude that DNA damage is not necessary for ZBTB38 to accumulate upon H_2O_2 treatment.

We also monitored the levels of ZBTB38 protein, phospho-H2AX and ROS in cells exposed to hydroxyurea and etoposide, which cause different types of DNA lesions. Under the conditions used, both drugs increased the level of phospho-H2AX but not the levels of cellular ROS (measured by dihydroethidium fluorescence, Figure 3C); the drugs also failed to cause ZBTB38 protein accumulation (Figure 3C). This demonstrates that DNA damage is not sufficient to cause ZBTB38 accumulation.

To confirm the role of H_2O_2-generated ROS on ZBTB38 protein stability, HeLa cells were treated with recombinant ROS-scavenging enzymes prior to H_2O_2 exposure (Figure 3D). Treatment with extracellular superoxide dismutase (SOD) or catalase failed to prevent ZBTB38 accumulation. However, when the enzymes were made cell-permeable by coupling to PEG, they prevented ZBTB38 accumulation in response to H_2O_2 (Figure 3D). Thus, ZBTB38 accumulation occurs as a result of an elevation of intracellular ROS levels. We also noticed that the USP9X protein was upregulated after treatment of the cells with H_2O_2, whereas another deubiquitinase, USP7, was not upregulated (Figure 3E).

Our following question was whether USP9X was required for ZBTB38 accumulation upon H_2O_2 treatment. The level of ZBTB38 protein was found to be very low in cells treated with siRNAs targeting USP9X, and the exposure to H_2O_2 did not induce ZBTB38 accumulation in these cells (Figure 3F). Pretreatment of the cells with the USP9X inhibitor WP1130 also blocked the accumulation of ZBTB38 upon addition of H_2O_2 (Figure 3G). These data indicate that the depletion of USP9X or the inhibition of its deubiquitinase activity prevents the accumulation of ZBTB38 induced by H_2O_2 exposure.

A proximity ligation assay further confirmed that USP9X and ZBTB38 interact in the nucleus upon H_2O_2 treatment (Supplementary Figure S3F). Finally, we noticed that gamma-irradiation, like H_2O_2 treatment, causes the accumulation of USP9X protein without altering the expression level of the other deubiquitinase found in the ZBTB38 complex, USP7 (Supplementary Figure S3G). Altogether these data suggest that USP9X and its deubiquitinase activity are necessary for ZBTB38 accumulation upon oxidative stress.

ZBTB38 and USP9X control the cellular response to H_2O_2 exposure in human cells, and they are part of the same pathway

The accumulation of USP9X and ZBTB38 upon H_2O_2 exposure suggested that these proteins might play a functional role in the response to ROS, so we next performed survival assays. First, cells were treated with siRNAs directed against ZBTB38 and/or USP9X prior to H_2O_2 exposure, then cell viability was monitored by a trypan blue exclusion assay. The H_2O_2 treatment caused little lethality in control cells (Figure 4A). In line with our previous observations (12), we found that knocking down ZBTB38 in unstressed cells had no detectable effect on viability; in contrast, cells depleted of ZBTB38 were significantly more sensitive to H_2O_2-induced killing (Figure 4A), and so were

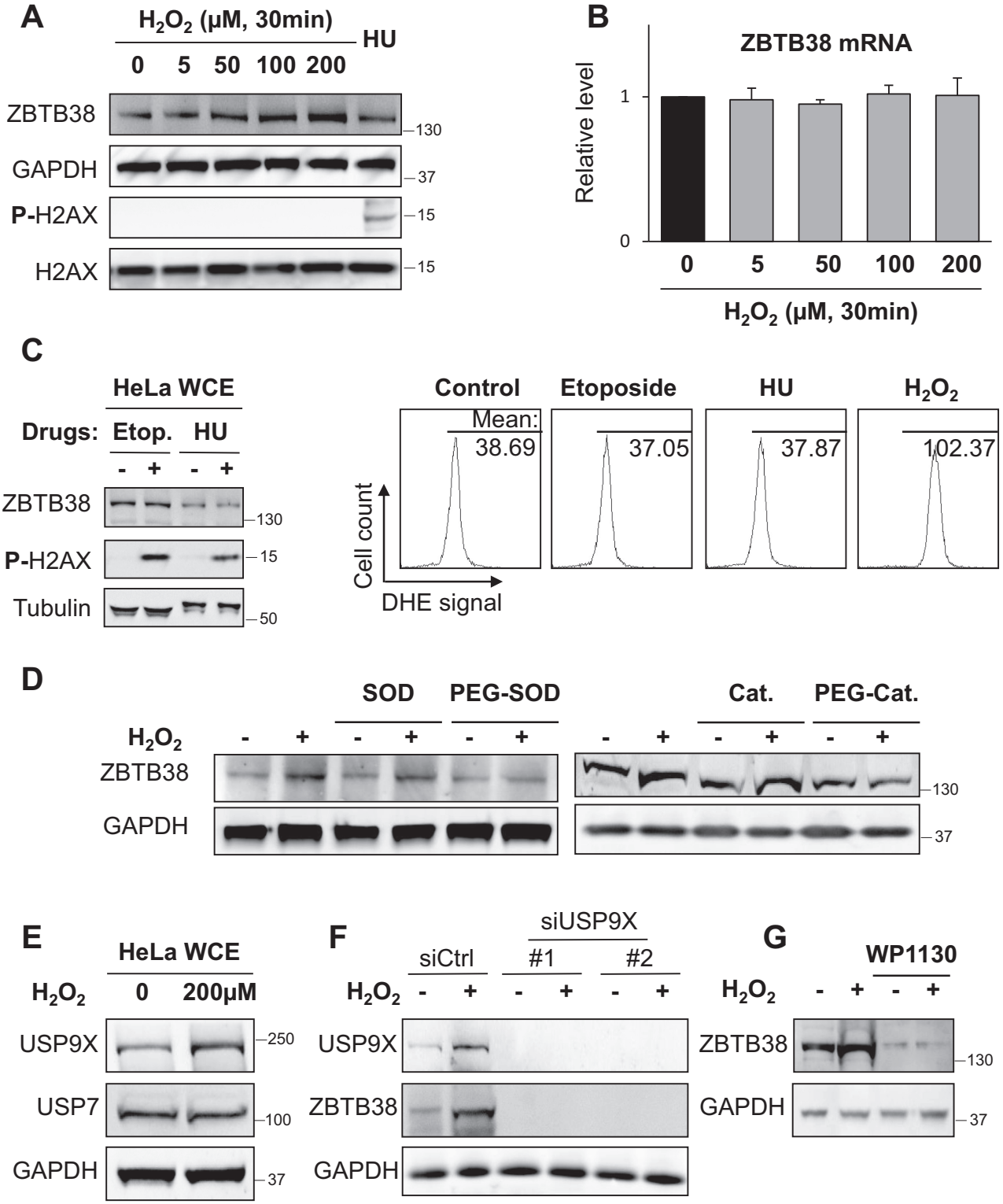

Figure 3. The ZBTB38 protein accumulates in H_2O_2-treated cells, and the accumulation depends on ROS and USP9X activity. (**A**) Western blot analysis in HeLa cells exposed to H_2O_2 at the indicated concentrations for 30 min. **P**-H2AX: phosphorylated H2AX. Hydroxyurea treatment (HU) was used as a positive condition for H2AX phosphorylation. (**B**) ZBTB38 mRNA levels in samples from panel A. qRT-PCR normalized with three housekeeping genes (MAPK14, TBP and TFRC), $n = 3$. (**C**) Left panel: treatment of HeLa cells with Etoposide (Etop.; 200 μM for 1 h) or Hydroxyurea (HU; 2 mM for 2 h) causes DNA damage, but no ZBTB38 accumulation. Right panel: Etoposide or Hydroxyurea do not increase the intracellular ROS levels, as measured by DHE staining. The mean DHE intensity is indicated on the graph. (**D**) Extracellular Superoxide Dismutase (SOD) or Catalase (Cat.) do not prevent ZBTB38 accumulation in response to H_2O_2 treatment (200 μM for 30 min), but PEG-coupled SOD or Cat., which are cell-permeable, do prevent ZBTB38 accumulation. (**E**) USP9X, but not USP7, accumulates in cells treated with H_2O_2 (200 μM for 30 min). (**F**) ZBTB38 protein does not accumulate in response to H_2O_2 in cells depleted of UPS9x. (**G**) Inhibition of USP9X by WP1130 prevents ZBTB38 accumulation in response to H_2O_2 treatment.

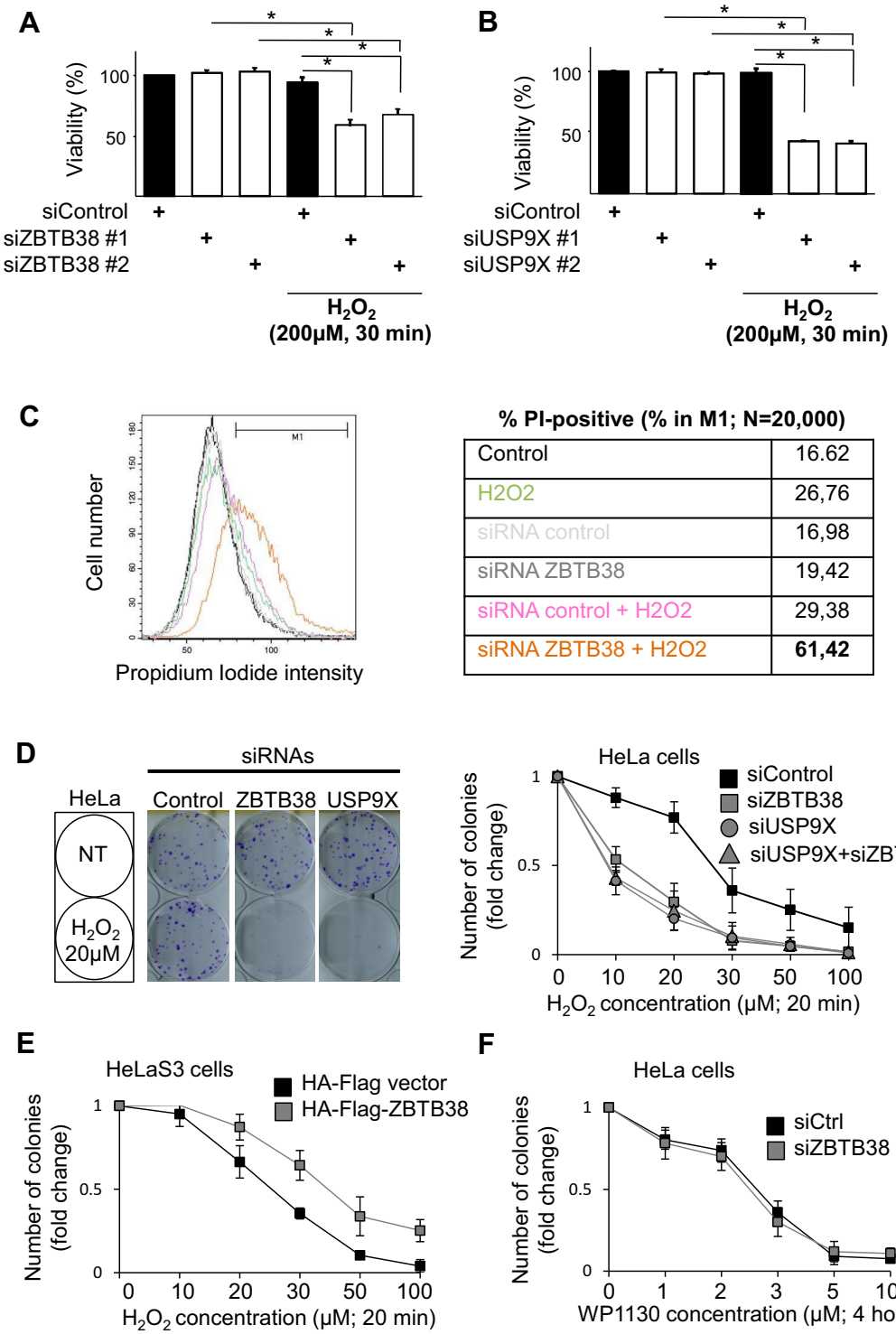

Figure 4. ZBTB38 and USP9X protect cells against H2O2-induced cell death. (**A**) Depletion of ZBTB38 by siRNAs sensitizes HeLa cell to killing by H_2O_2 (200 µM, 30 min). Cell viability 12 h after treatment was determined by trypan blue staining and reported as % viability = (total cells – positive cells)/total cells; three independent experiments are plotted on the graph (±S.E.M.) Student's *t*-test; in all figures: * indicates $P < 0.05$; ** indicates $P < 0.01$; *** indicates $P < 0.001$; NS indicates no statistical significance. (**B**) Depletion of USP9X also sensitizes HeLa cells to killing by H_2O_2. Legend as in panel A. (**C**) As in A, but cell viability was measured by FACS, using a propidium iodide (PI) intake assay on 20,000 cells. The graphs are shown on the left panel, and the median value of the PI-intensity is reported in the table on the right. (**D**) Combined depletion of ZBTB38 and USP9X has no greater effect than either single depletion. As in A and B, but the effect of ZBTB38 and USP9X depletion on H_2O_2 sensitivity was tested by counting colonies 15 days after the treatment. Left panel: representative images of wells. Right panel: quantification of colony number for the indicated siRNA transfections and H_2O_2 concentrations. (**E**) The HeLa cell line expressing exogenous HA-Flag-ZBTB38 is more resistant to H_2O_2 than its counterpart containing an empty expression vector. Colony formation assay as in panel D. (**F**) HeLa cells are sensitive to killing by WP1130, and depleting ZBTB38 does not cause increased sensitivity. Colony formation assay as in panel D.

cells depleted of USP9X (Figure 4B). The hypersensitivity of ZBTB38-depleted cells to H_2O_2 was confirmed using two additional methods: propidium iodide intake measurement by FACS (Figure 4C) and colony formation assays (Figure 4D). Using the trypan blue exclusion assay, we also observed that ZBTB38-depleted cells were more sensitive than controls to an exposure to IR (Supplementary Figure S4A), but not to hydroxyurea (Supplementary Figure S4B) or etoposide (Supplementary Figure S4C), consistent with a specific role of ZBTB38 in responding to oxidative stress rather than DNA damage. In agreement with this hypothesis, the HA-Flag-ZBTB38 cell line, which expresses ∼1.5x-fold more ZBTB38 than its unmodified counterpart, was more resistant to H_2O_2 (Figure 4E).

We next investigated whether USP9X and ZBTB38 may act in the same pathway. The survival of cells treated with siRNAs against ZBTB38, USP9X, or both, was monitored upon H_2O_2 exposure. In different cell types, we observed that depletion of USP9X or ZBTB38 reduced the colony-forming potential of H_2O_2-treated cells (Figure 4D, Supplementary Figure S4D, and S4E). The combined depletion of USP9X and ZBTB38 did not have a greater effect than the individual depletions (Figure 4D, Supplementary Figure S4D and E). A final argument supporting epistasy is that ZBTB38-depleted cells were not more sensitive than control cells to the toxic effects of WP1130 inhibition (Figure 4F, Supplementary Figure S4F and G).

From these results we conclude that USP9X and ZBTB38 both contribute to cell survival upon oxidative stress, and that they act in the same pathway.

Depletion of ZBTB38 increases cellular ROS level and modifies the cellular response to ROS

We next sought to understand how ZBTB38 and USP9X may affect the cellular sensitivity to ROS.

First, using DHE labelling, we determined the cellular level of ROS following a depletion of ZBTB38 or USP9X in HeLa cells. The DHE fluorescence value was significantly higher in cells depleted of ZBTB38 or USP9X than in control cells (Figure 5A and B). We note that the effect of ZBTB38 or USP9X depletion was smaller in magnitude than the effect caused by exposure to 200 μM H_2O_2 (Figure 5A and B). The effect was also specific, as it did not occur upon knockdown of unrelated methyl-CpG binding proteins (UHRF1 and UHRF2) or of a different deubiquitinase, USP7 (Figure 5B). Finally, the fact that ZBTB38 knockdown caused an increase in ROS was confirmed using a different indicator dye, DCF-DA, and was observed in different cell lines (Supplementary Figure S5A).

We next sought to understand how ZBTB38 depletion may cause an increase of ROS in cells. Using qRT-PCR, we measured the expression of two important cellular factors in ROS homeostasis and response: c-Myc (25) and AMPK (26)—they were not modified by ZBTB38 knockdown (Supplementary Figure S5B). The GSH/GSSG ratio, the amount of mitochondrial DNA, and the antioxidant activity were not modified either by ZBTB38 knockdown (Supplementary Figure S5C); this rules out a number of possibilities by which ZBTB38 depletion could lead to increased ROS abundance.

Three functionally important proteins induced by H_2O_2 were also monitored: NRF2, SIRT1, and PGC1-alpha (27–29). As expected, H_2O_2 treatment at this dose (400 μM, 20 minutes) induced the phosphorylation of H2AX, as well as the induction of NRF2, SIRT1 and PGC1-alpha (Figure 5C). In contrast, the depletion of ZBTB38 by siRNA was not sufficient to elicit any of these responses (Figure 5C).

Cells that were challenged by H_2O_2 after ZBTB38 depletion were also examined; in this condition we observed striking defects. Indeed, in the absence of ZBTB38, H_2O_2 treatment failed to induce NRF2 expression (Figure 5C). On the other hand H2AX phosphorylation, a mark of DNA damage, was higher in ZBTB38-depleted cells than in control cells (Figure 5C). These data indicate that, in the absence of ZBTB38, the NRF2 signaling pathway triggered by H_2O_2 exposure is not properly regulated.

DISCUSSION

We report the identification of a new molecular pathway that responds to ROS, limits their endogenous generation, and counteracts their toxic effect. The pathway links a deubiquitinase, USP9X, and a methyl-CpG-binding transcriptional regulator, ZBTB38.

ZBTB38: a new nuclear target of USP9X

Three USP9X-associated complexes have been previously characterized (30–32). ZBTB38 was not detected in any of these, and conversely these complexes show very little overlap with the ZBTB38 complex we have isolated (data not shown). This could be explained by the fact that these previous studies were performed on total cellular extracts and that USP9X is mostly located in the cytoplasm; therefore most USP9X interactors reported so far are cytoplasmic (33). In the nucleus, USP9X has been found to interact with a handful of transcription factors including Oct4, ERG, FOXO3A and SOX2 (34–37). None of these transcription factors were detected in our ZBTB38 complexes, leading us to the idea that USP9X forms a distinct nuclear complex with ZBTB38.

USP9X binds certain targets (e.g. ASK1) through the recognition of a Glycine-Glycine motif, also present in Ubiquitin (38–41). We found a GG motif at position 799 of human ZBTB38, within the USP9X-interacting domain identified by pull-down. This motif is conserved in many vertebrates, suggesting that it could potentially mediate the interaction.

We have previously established that ZBTB38 is ubiquitinated and destabilized by the E3 ligase RBBP6 (12). Here we show that USP9X has the converse effect—deubiquitination and stabilization of ZBTB38—even when RBBP6 is overexpressed, therefore it is possible that the two enzymes act antagonistically on the same residues. K804, a conserved lysine residue in ZBTB38 has been experimentally shown to be subject to ubiquitination (42), and other residues (K308, K754, K964), have high prediction scores as ubiquitin acceptors. These residues are potential candidates for deubiquitination by USP9X. The type of ubiquitin chains present on ZBTB38 is currently unknown, but it could possibly

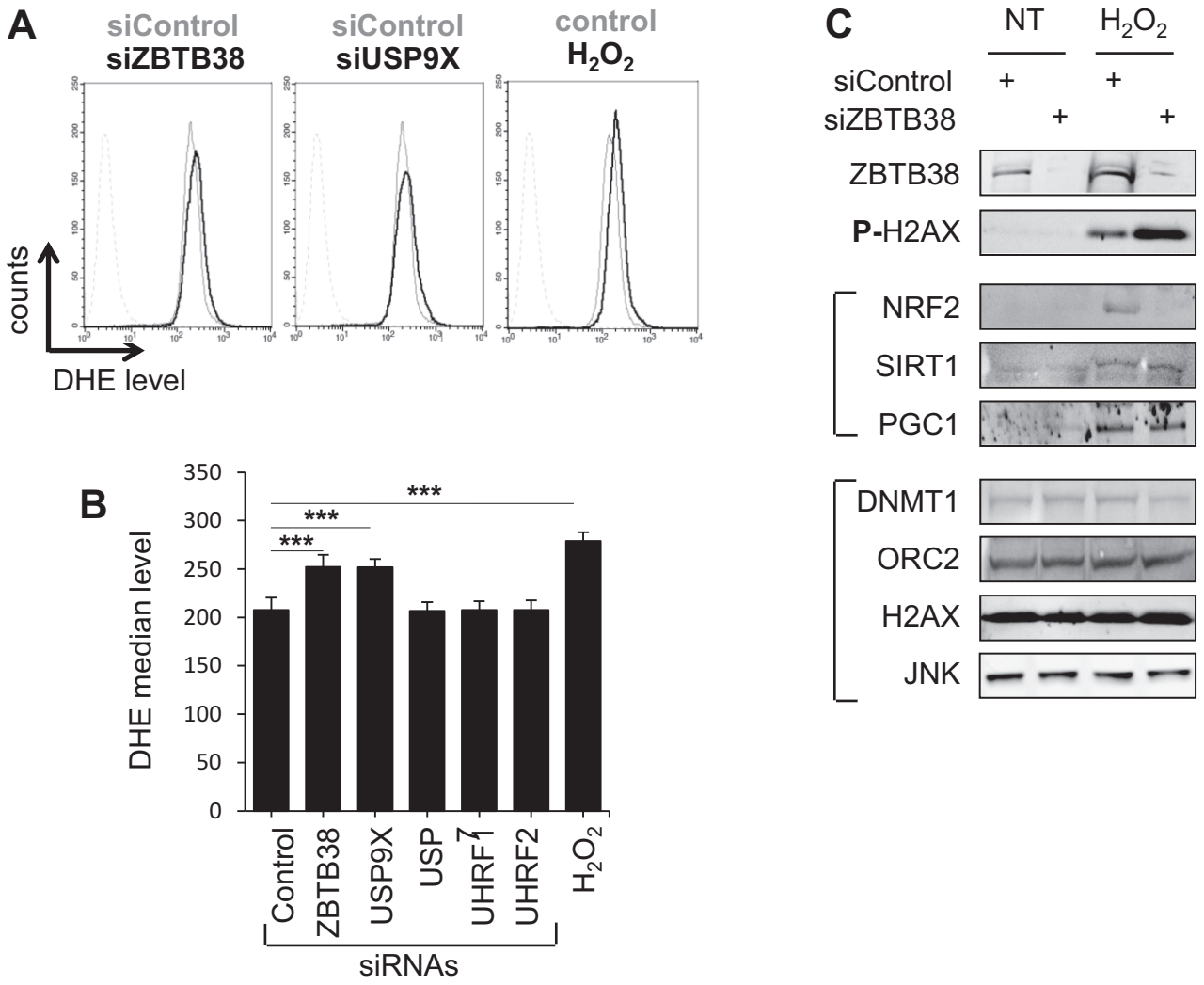

Figure 5. Depletion of ZBTB38 increases ROS levels and modifies the response to oxidative stress. (**A**) FACS analysis of DHE intensity level in cells treated with siRNAs against ZBTB38 or USP9X, compared to cells treated with H_2O_2. Twenty-four hours after transfection of the siRNAs, cells were stained live with DHE (1 mM final) for 20 min in phosphate buffered saline solution and directly analyzed by FACS; 20 000 cells were analyzed per condition. (**B**) Quantification of panel A, also including additional siRNAs, $n = 3$, Student's t-test. (**C**) Western blot analysis of the expression of different markers of oxidative stress in ZBTB38-depleted cells subjected or not to H_2O_2 exposure (400 μM for 20 min).

include K29, K48 or K63 linkages, all of which can be targeted by USP9X.

USP9X and ZBTB38 are essential for cell survival upon oxidative damage

Here, we demonstrate that upon H_2O_2 treatment both USP9X and ZBTB38 accumulate in cells, and that depletion of either protein by siRNA potentiates the deleterious effect of H_2O_2.

At first sight, these results contrast with previously reported observations: it has been shown that, upon H_2O_2 treatment, USP9X stabilizes ASK1, which in turn activates JNK and p38 signaling, eventually leading to cell death (41). In these experiments then, USP9X does not protect against, but instead sensitizes to death caused by oxidative stress.

A very likely explanation for this apparent discrepancy lies in the level of H_2O_2 applied to the cell. Nagai and colleagues used very high concentrations of H_2O_2 (1–10 mM, duration 15–120 min) designed to cause the formation of the ASK1 signalosome and cell death, whereas we used milder treatments (0.2 mM at most, 30 minutes or less) that caused little lethality in control cells. We note that the interaction of USP9X with ZBTB38 exists even in unstressed cells, whereas its interaction with ASK1 only occurs upon harsh H_2O_2 treatment (41). It is thus possible that USP9X promotes or prevents H_2O_2-triggered cell death by acting on different targets at varying levels of oxidative damage.

Both ZBTB38 and USP9X are expressed, at least at the RNA level, in a broad range of human organs (43), possibly hinting at a widespread relevance of the protective mechanism we have uncovered. We note that ZBTB38 is most expressed in the brain, an organ that is both critically sensitive to oxidative stress and dependent on USP9X function (44–45). Therefore, we speculate that the USP9X/ZBTB38 axis could be important for cerebral homeostasis relative to ox-

idative stress, but this would require further experiments to fully assess.

Relevance to cancer and chemotherapy

Besides the physiological settings discussed above, the mechanisms reported here may be important in the context of cancer and chemotherapy. Indeed USP9X has been shown to be a promising target for treatment: its inhibitor WP1130 (also known as Degrasyn) has clear anti-tumoral activity (24,46). Interestingly, WP1130 sensitizes cancer cells to other chemotherapeutic approaches, and the destabilization of ZBTB38 following WP1130 may play a role in these effects.

Lastly, it has been shown that oxidative stress plays an important role in prostate cancer (47), therefore the association between higher-expressing ZBTB38 SNPs and increased prostate cancer risk might rely on resistance to oxidative stress.

Possible mechanisms

Our data show that USP9X acts upstream of ZBTB38 to promote resistance to oxidative stress. Three mechanistic questions are of interest for future studies. First, how is this axis activated in the presence of oxidative stress? We have observed that USP9X protein abundance increases upon oxidative stress, so one possibility is that USP9X is subject to downregulation by KEAP1, an adaptor protein for E3 ubiquitin ligases which plays key roles in ROS response, and is itself destabilized upon oxidative stress (48). This increase in USP9X abundance would then lead to the increase in ZBTB38 protein abundance.

The second question is: why does the lack of ZBTB38 lead to increased ROS levels in basal conditions? In vitro, ZBTB38 has preferential affinity for two different sets of methylated consensus sequences, which it binds through two different sets of Zinc fingers (10–11). As ZBTB38 represses transcription (9,12,22,49), its role against oxidative stress could entail dampening the expression of methylated genes. Potential candidates include genes regulating the production of ROS by mitochondria, and their detoxification. ChIP-Seq in a relevant biological system would be one possibility to identify these genes in the future.

The last question is: why does ZBTB38 knockdown lead to increased sensitivity upon a challenge with oxidative stress? A striking observation is that cells lacking ZBTB38 fail to show high NRF2 induction upon oxidative stress. NRF2 activates a ROS detoxifying program (48), so the diminished NRF2 response could explain part of the ROS sensitivity of cells lacking ZBTB38. Future experiments will help investigate this possibility.

SUPPLEMENTARY DATA

Supplementary Data are available at NAR Online.

ACKNOWLEDGEMENTS

P.A.D. thanks Allison Bardin, David Bernard and Saadi Khochbin for advice and useful comments on the paper. P.A.D. thanks Slimane Ait-si-ali for help with proteomics, in addition to Joe Card for processing TAP-MS samples.

FUNDING

Labex 'Who am I?' [ANR-11-LABX-0071, ANR-11-IDEX-005-02 to B.M. and P.A.D.]; Electricité de France [123518 to B.M.]; Ligue contre le cancer Comité de Paris [RS11/75-81, RS12/75/95-21, RS13/75-59 to B.M.]; FP7 Marie Curie action [PIRG07-GA-2010-268448 to B.M.]; Fondation pour la Recherche Médicale [AJE20151234749 to B.M., FDT20150532354 to C.M.]; Institut National du Cancer [ASC15018KSA to B.M., INCa PLBio 2015-1-PLBio-01-DR A-1 to P.A.D.]; Institut Cochin [POC2016 to B.M.]; AFM-Téléthon [17167 to P.A.D.]; Association pour la Recherche contre le Cancer [ARC2014 to P.A.D.]; Agence Nationale de la Recherche [ANR-15-CE12-0012-01 to P.A.D.]; the Dana-Farber Strategic Research Initiative (to J.A.M.); National Institutes of Health [CA203655, CA215489 to J.A.M.]. The open access publication charge for this paper has been waived by Oxford University Press - *NAR* Editorial Board members are entitled to one free paper per year in recognition of their work on behalf of the journal.

Conflict of interest statement. None declared.

REFERENCES

1. Sies,H., Berndt,C. and Jones,D.P. (2017) Oxidative Stress. *Annu. Rev. Biochem.*, **86**, 715–748.
2. Schäfer,M. and Werner,S. (2015) Nrf2—a regulator of keratinocyte redox signaling. *Free Radic. Biol. Med.*, **88**, 243–252.
3. Nathan,C. and Cunningham-Bussel,A. (2013) Beyond oxidative stress: an immunologist's guide to reactive oxygen species. *Nat. Rev. Immunol.*, **13**, 349–361.
4. Taguchi,K., Motohashi,H. and Yamamoto,M. (2011) Molecular mechanisms of the Keap1–Nrf2 pathway in stress response and cancer evolution. *Genes Cells*, **16**, 123–140.
5. Murakami,S. and Motohashi,H. (2015) Roles of Nrf2 in cell proliferation and differentiation. *Free Radic. Biol. Med.*, **88**, 168–178.
6. Valinluck,V., Tsai,H.-H., Rogstad,D.K., Burdzy,A., Bird,A. and Sowers,L.C. (2004) Oxidative damage to methyl-CpG sequences inhibits the binding of the methyl-CpG binding domain (MBD) of methyl-CpG binding protein 2 (MeCP2). *Nucleic Acids Res.*, **32**, 4100–4108.
7. Lister,R., Pelizzola,M., Dowen,R.H., Hawkins,R.D., Hon,G., Tonti-Filippini,J., Nery,J.R., Lee,L., Ye,Z., Ngo,Q.-M. *et al.* (2009) Human DNA methylomes at base resolution show widespread epigenomic differences. *Nature*, **462**, 315–322.
8. Geiger,T., Wehner,A., Schaab,C., Cox,J. and Mann,M. (2012) Comparative proteomic analysis of eleven common cell lines reveals ubiquitous but varying expression of most proteins. *Mol. Cell Proteomics*, **11**, M111.014050.
9. Filion,G.J.P., Zhenilo,S., Salozhin,S., Yamada,D., Prokhortchouk,E. and Defossez,P.-A. (2006) A family of human zinc finger proteins that bind methylated DNA and repress transcription. *Mol. Cell. Biol.*, **26**, 169–181.
10. Sasai,N., Nakao,M. and Defossez,P.-A. (2010) Sequence-specific recognition of methylated DNA by human zinc-finger proteins. *Nucleic Acids Res.*, **38**, 5015–5022.
11. Pozner,A., Hudson,N.O., Trewhella,J., Terooatea,T.W., Miller,S.A. and Buck-Koehntop,B.A. (2017) The C-terminal zinc fingers of ZBTB38 are novel selective readers of DNA methylation. *J. Mol. Biol.*, **430**, 258–271.
12. Miotto,B., Chibi,M., Xie,P., Koundrioukoff,S., Moolman-Smook,H., Pugh,D., Debatisse,M., He,F., Zhang,L. and Defossez,P.-A. (2014) The RBBP6/ZBTB38/MCM10 axis regulates DNA replication and common fragile site stability. *Cell Rep.*, **7**, 575–587.
13. Kote-Jarai,Z., Olama,A.A.A., Giles,G.G., Severi,G., Schleutker,J., Weischer,M., Campa,D., Riboli,E., Key,T., Gronberg,H. *et al.* (2011) Seven prostate cancer susceptibility loci identified by a multi-stage genome-wide association study. *Nat. Genet.*, **43**, 785–791.

14. Ferry,L., Fournier,A., Tsusaka,T., Adelmant,G., Shimazu,T., Matano,S., Kirsh,O., Amouroux,R., Dohmae,N., Suzuki,T. *et al.* (2017) Methylation of DNA Ligase 1 by G9a/GLP Recruits UHRF1 to Replicating DNA and Regulates DNA Methylation. *Mol. Cell*, **67**, 550–565.
15. Adelmant,G., Calkins,A.S., Garg,B.K., Card,J.D., Askenazi,M., Miron,A., Sobhian,B., Zhang,Y., Nakatani,Y., Silver,P.A. *et al.* (2012) DNA ends alter the molecular composition and localization of Ku multicomponent complexes. *Mol. Cell Proteomics*, **11**, 411–421.
16. Ficarro,S.B., Zhang,Y., Lu,Y., Moghimi,A.R., Askenazi,M., Hyatt,E., Smith,E.D., Boyer,L., Schlaeger,T.M., Luckey,C.J. *et al.* (2009) Improved electrospray ionization efficiency compensates for diminished chromatographic resolution and enables proteomics analysis of tyrosine signaling in embryonic stem cells. *Anal. Chem.*, **81**, 3440–3447.
17. Askenazi,M., Parikh,J.R. and Marto,J.A. (2009) mzAPI: a new strategy for efficiently sharing mass spectrometry data. *Nat. Methods*, **6**, 240–241.
18. Rozenblatt-Rosen,O., Deo,R.C., Padi,M., Adelmant,G., Calderwood,M.A., Rolland,T., Grace,M., Dricot,A., Askenazi,M., Tavares,M. *et al.* (2012) Interpreting cancer genomes using systematic host network perturbations by tumour virus proteins. *Nature*, **487**, 491–495.
19. Laget,S., Miotto,B., Chin,H.G., Estève,P.-O., Roberts,R.J., Pradhan,S. and Defossez,P.-A. (2014) MBD4 cooperates with DNMT1 to mediate methyl-DNA repression and protects mammalian cells from oxidative stress. *Epigenetics*, **9**, 546–556.
20. Baymaz,H.I., Fournier,A., Laget,S., Ji,Z., Jansen,P.W.T.C., Smits,A.H., Ferry,L., Mensinga,A., Poser,I., Sharrocks,A. *et al.* (2014) MBD5 and MBD6 interact with the human PR-DUB complex through their methyl-CpG-binding domain. *Proteomics*, **14**, 2179–2189.
21. Kasibhatla,S., Amarante-Mendes,G.P., Finucane,D., Brunner,T., Bossy-Wetzel,E. and Green,D.R. (2006) Propidium iodide (PI) uptake assay to detect apoptosis. *CSH Protoc*, **2006**, pdb.prot4495.
22. Oikawa,Y., Omori,R., Nishii,T., Ishida,Y., Kawaichi,M. and Matsuda,E. (2011) The methyl-CpG-binding protein CIBZ suppresses myogenic differentiation by directly inhibiting myogenin expression. *Cell Res.*, **21**, 1578–1590.
23. Li,Z., Cheng,Z., Raghothama,C., Cui,Z., Liu,K., Li,X., Jiang,C., Jiang,W., Tan,M., Ni,X. *et al.* (2017) USP9X controls translation efficiency via deubiquitination of eukaryotic translation initiation factor 4A1. *Nucleic Acids Res.*, **46**, 823–839.
24. Kapuria,V., Peterson,L.F., Fang,D., Bornmann,W.G., Talpaz,M. and Donato,N.J. (2010) Deubiquitinase inhibition by small-molecule WP1130 triggers aggresome formation and tumor cell apoptosis. *Cancer Res.*, **70**, 9265–9276
25. Vafa,O., Wade,M., Kern,S., Beeche,M., Pandita,T.K., Hampton,G.M. and Wahl,G.M. (2002) c-Myc can induce DNA damage, increase reactive oxygen species, and mitigate p53 function: a mechanism for oncogene-induced genetic instability. *Mol. Cell*, **9**, 1031–1044.
26. Mungai,P.T., Waypa,G.B., Jairaman,A., Prakriya,M., Dokic,D., Ball,M.K. and Schumacker,P.T. (2011) Hypoxia triggers AMPK activation through reactive oxygen species-mediated activation of calcium release-activated calcium channels. *Mol. Cell. Biol.*, **31**, 3531–3545.
27. Nguyen,T., Nioi,P. and Pickett,C.B. (2009) The Nrf2-antioxidant response element signaling pathway and its activation by oxidative stress. *J. Biol. Chem.*, **284**, 13291–13295.
28. O'Hagan,H.M., Wang,W., Sen,S., Destefano Shields,C., Lee,S.S., Zhang,Y.W., Clements,E.G., Cai,Y., Van Neste,L., Easwaran,H. *et al.* (2011) Oxidative damage targets complexes containing DNA methyltransferases, SIRT1, and polycomb members to promoter CpG Islands. *Cancer Cell*, **20**, 606–619.
29. St-Pierre,J., Drori,S., Uldry,M., Silvaggi,J.M., Rhee,J., Jäger,S., Handschin,C., Zheng,K., Lin,J., Yang,W. *et al.* (2006) Suppression of reactive oxygen species and neurodegeneration by the PGC-1 transcriptional coactivators. *Cell*, **127**, 397–408.
30. Trinkle-Mulcahy,L., Boulon,S., Lam,Y.W., Urcia,R., Boisvert,F.-M., Vandermoere,F., Morrice,N.A., Swift,S., Rothbauer,U., Leonhardt,H. *et al.* (2008) Identifying specific protein interaction partners using quantitative mass spectrometry and bead proteomes. *J. Cell Biol.*, **183**, 223–239.
31. Agrawal,P., Chen,Y.-T., Schilling,B., Gibson,B.W. and Hughes,R.E. (2012) Ubiquitin-specific peptidase 9, X-linked (USP9X) modulates activity of mammalian target of rapamycin (mTOR). *J. Biol. Chem.*, **287**, 21164–21175.
32. Han,K.-J., Foster,D.G., Zhang,N.-Y., Kanisha,K., Dzieciatkowska,M., Sclafani,R.A., Hansen,K.C., Peng,J. and Liu,C.-W. (2012) Ubiquitin-specific protease 9x deubiquitinates and stabilizes the spinal muscular atrophy protein-survival motor neuron. *J. Biol. Chem.*, **287**, 43741–43752.
33. Murtaza,M., Jolly,L.A., Gecz,J. and Wood,S.A. (2015) La FAM fatale: USP9X in development and disease. *Cell. Mol. Life Sci.*, **72**, 2075–2089.
34. van den Berg,D.L.C., Snoek,T., Mullin,N.P., Yates,A., Bezstarosti,K., Demmers,J., Chambers,I. and Poot,R.A. (2010) An Oct4-centered protein interaction network in embryonic stem cells. *Cell Stem Cell*, **6**, 369–381.
35. Cox,J.L., Wilder,P.J., Gilmore,J.M., Wuebben,E.L., Washburn,M.P. and Rizzino,A. (2013) The SOX2-interactome in brain cancer cells identifies the requirement of MSI2 and USP9X for the growth of brain tumor cells. *PLoS ONE*, **8**, e62857.
36. Zheng,X., Zhai,B., Koivunen,P., Shin,S.J., Lu,G., Liu,J., Geisen,C., Chakraborty,A.A., Moslehi,J.J., Smalley,D.M. *et al.* (2014) Prolyl hydroxylation by EglN2 destabilizes FOXO3a by blocking its interaction with the USP9x deubiquitinase. *Genes Dev.*, **28**, 1429–1444.
37. Wang,S., Kollipara,R.K., Srivastava,N., Li,R., Ravindranathan,P., Hernandez,E., Freeman,E., Humphries,C.G., Kapur,P., Lotan,Y. *et al.* (2014) Ablation of the oncogenic transcription factor ERG by deubiquitinase inhibition in prostate cancer. *Proc. Natl. Acad. Sci. U.S.A.*, **111**, 4251–4256.
38. Amerik,A.Y. and Hochstrasser,M. (2004) Mechanism and function of deubiquitinating enzymes. *Biochim. Biophys. Acta*, **1695**, 189–207.
39. Komander,D., Lord,C.J., Scheel,H., Swift,S., Hofmann,K., Ashworth,A. and Barford,D. (2008) The structure of the CYLD USP domain explains its specificity for Lys63-linked polyubiquitin and reveals a B box module. *Mol. Cell*, **29**, 451–464.
40. Messick,T.E., Russell,N.S., Iwata,A.J., Sarachan,K.L., Shiekhattar,R., Shanks,J.R., Reyes-Turcu,F.E., Wilkinson,K.D. and Marmorstein,R. (2008) Structural basis for ubiquitin recognition by the Otu1 ovarian tumor domain protein. *J. Biol. Chem.*, **283**, 11038–11049.
41. Nagai,H., Noguchi,T., Homma,K., Katagiri,K., Takeda,K., Matsuzawa,A. and Ichijo,H. (2009) Ubiquitin-like sequence in ASK1 plays critical roles in the recognition and stabilization by USP9X and oxidative stress-induced cell death. *Mol. Cell*, **36**, 805–818.
42. Kim,W., Bennett,E.J., Huttlin,E.L., Guo,A., Li,J., Possemato,A., Sowa,M.E., Rad,R., Rush,J., Comb,M.J. *et al.* (2011) Systematic and quantitative assessment of the ubiquitin-modified proteome. *Mol. Cell*, **44**, 325–340.
43. GTEx Consortium (2013) The Genotype-Tissue Expression (GTEx) project. *Nat. Genet.*, **45**, 580–585.
44. Soga,M., Matsuzawa,A. and Ichijo,H. (2012) Oxidative stress-induced diseases via the ASK1 signaling pathway. *Int. J. Cell Biol.*, **2012**, 439587.
45. Stegeman,S., Jolly,L.A., Premarathne,S., Gecz,J., Richards,L.J., Mackay-Sim,A. and Wood,S.A. (2013) Loss of Usp9x disrupts cortical architecture, hippocampal development and TGFβ-mediated axonogenesis. *PLoS ONE*, **8**, e68287.
46. Bartholomeusz,G., Talpaz,M., Bornmann,W., Kong,L.-Y. and Donato,N.J. (2007) Degrasyn activates proteasomal-dependent degradation of c-Myc. *Cancer Res.*, **67**, 3912–3918.
47. Kumar,B., Koul,S., Khandrika,L., Meacham,R.B. and Koul,H.K. (2008) Oxidative stress is inherent in prostate cancer cells and is required for aggressive phenotype. *Cancer Res.*, **68**, 1777–1785.
48. Suzuki,T. and Yamamoto,M. (2017) Stress-sensing mechanisms and the physiological roles of the Keap1-Nrf2 system during cellular stress. *J. Biol. Chem.*, **292**, 16817–16824.
49. Kotoku,T., Kosaka,K., Nishio,M., Ishida,Y., Kawaichi,M. and Matsuda,E. (2016) CIBZ regulates mesodermal and cardiac differentiation of by suppressing T and Mesp1 expression in mouse embryonic Stem Cells. *Sci. Rep.*, **6**, 34188.